Analysis of the single toggle jaw crusher kinematics

Moses Frank Oduori, Stephen Mwenje Mutuli and David Masinde Munyasi
Department of Mechanical and Manufacturing Engineering, The University of Nairobi, Nairobi, Kenya

Received 10 January 2013
Revised 22 July 2013
Accepted 13 August 2013

Abstract

Purpose – This paper aims to obtain equations that can be used to describe the motion of any given point in the swing jaw of a single toggle jaw crusher.

Design/methodology/approach – The swing jaw drive mechanism of a single toggle jaw crusher is modelled as a planar crank and rocker mechanism with the swing jaw as the coupler link. Starting with the vector loop closure equation for the mechanism, equations of the position, velocity and acceleration of any given point in the swing jaw are obtained.

Findings – Application of the kinematical equations that were obtained is demonstrated using the dimensional data of a practical single toggle jaw crusher. Thus, a description of the kinematics of any given point in the swing jaw of a single toggle jaw crusher is realized.

Originality/value – The model of the single toggle jaw crusher mechanism as a planar crank and rocker mechanism is a realistic one. The equations obtained in this paper should be useful in further studies on the mechanics and design of the single toggle jaw crusher.

Keywords Model, Crusher, Jaw, Kinematical, Single, Toggle

Paper type Research paper

Introduction

The jaw crusher is versatile, and it can be used to crush rocks, whose hardness may range from medium-hard to extremely hard, as well as different kinds of ore, building rubble and glass, among other hard materials. It is widely used in a variety of demolition, extraction, reclamation and recycling industries, but especially, in the mining and construction sectors (AUBEMA Jaw Crushers, 2013; SBM Mining and Construction Machinery, 2013).

The heart of the crushing mechanism of a jaw crusher consists of two metallic jaw plates that are slightly and oppositely inclined away from the vertical to form a V-shaped crushing zone with a wide upper opening and a narrow lower opening. One of the jaw plates is fixed, whereas the other is movable and referred to as the swing jaw. When in operation, the charge of material to be crushed is fed into the crushing zone through the upper opening. The swing jaw is driven to execute a cyclic reversing motion and to apply cyclic intermittent compressive forces that crush the charge of material against the fixed jaw. As the larger lumps of material are crushed into smaller lumps, they fall, under gravity, into the narrower lower sections of the crushing zone, where they are crushed again into even smaller lumps. This process is repeated until the charge of material is all crushed into aggregates that are small enough to fall out of the crusher, through the opening at the lower end of the crushing zone (Gupta and Yan, 2006). The crushing mechanism is enclosed in a box-like steel frame.

Journal of Engineering, Design and Technology
Vol. 13 No. 2, 2015
pp. 213-239

1726-0531
DOI 10.1108/JEDT-01-2013-0001

The jaw crusher can be crawler track-mounted or trailer-mounted to realize a mobile unit that can be repositioned, when the need arises, even as the work advances. Moreover, in many cases, the jaw crusher can be easily disassembled for relocation or access to confined places (Carter, 1999). This enables the jaw crusher to be used in both surface and underground mining. Other advantages of the jaw crusher include its simplicity in structure and mechanism, reliability, ease of maintenance and high capacity, as compared to other types of crusher, such as the cone crusher, the gyratory crusher and the various designs of impact crushers (Zhong and Chen, 2010).

Today, the most commonly used types of jaw crusher are the single toggle and the double toggle designs. The original double toggle jaw crusher was designed by Eli Whitney Blake in the USA in 1857 (Mular *et al.*, 2002). The motion of the swing jaw in a double toggle crusher is such that it applies an almost purely compressive force upon the material being crushed. This minimizes wear on the crushing surfaces of the jaws and makes the double toggle jaw crusher suitable for crushing highly abrasive and very hard materials. Even today, the Blake design, with some comparatively minor improvements, can still be found in mines and quarries around the world.

The single toggle design, which was developed between the 1920s and the 1950s, is a simpler, lighter crusher (Mular *et al.*, 2002). Its swing jaw has an elliptical rolling motion such that it applies a compressive as well as a rubbing force on the material being crushed. This has a force-feeding effect that improves the throughput of the device, but it also tends to cause rapid wear of the crushing surfaces of the jaws. However, the single toggle jaw crusher has a lower installed cost, as compared to the double toggle design. Improvements in materials and design have made the single toggle jaw crusher more common today as the primary crusher in quarrying operations (The Institute of Quarrying Australia, 2013). According to Carter (1999), sales of the single toggle jaw crusher exceed those of the double toggle jaw crusher by a factor of at least nine to one.

The crushing action of a jaw crusher is brought about by the motion of its swing jaw and the forces that it exerts on the material being crushed (Gupta and Yan, 2006; Pennsylvania Crusher Corporation, 2006). Therefore, in the study and design of the jaw crusher, it is important to understand the kinematics of the swing jaw.

This paper sets out to obtain a complete kinematical description of the single toggle jaw crusher, from first principles.

Literature review

The mechanics of the jaw crusher mechanism has caught the interest of authors for a long time (Ham *et al.*, 1958; Martin George, 1982; Erdman and Sandor, 1991). However, until recently (Cao *et al.*, 2006; Deepak, 2010), the literature on the kinematical analysis of jaw crushers of any kind, in general, and single toggle jaw crushers, in particular, has not been common to find.

Ham *et al.* (1958) discussed the double toggle jaw crusher as an example of a machine that utilizes the toggle effect to exert the large forces that are necessary for crushing hard rocks. They performed a static force analysis of the mechanism, but they did not perform a kinematical analysis. Likewise, Martin George (1982) also

featured the double toggle jaw crusher as an example of a toggle mechanism but did not perform a kinematical analysis or even a static force analysis of the mechanism.

Erdman and Sandor (1991) presented the double toggle stone crusher mechanism as an example problem, for the reader to solve by using the method of instant centres, and the method of complex numbers. They did not present a kinematical analysis of the mechanism from first principles.

The work of Cao *et al.* (2006) is a rare presentation of the kinematical analysis of the single toggle jaw crusher from first principles. The paper states kinematical equations without giving details of their derivation. Moreover, a substantial part of the paper by Cao *et al.* (2006) deals with the mechanism of fracture of the material being crushed, the wear of the crushing jaw surfaces, and it endeavours to explain these phenomena with regard to the kinematics of the swing jaw.

Deepak (2010) derived, in detail, the same kinematical equations that had been presented by Cao *et al.* (2006). Garnaik (2010) used the equations that had been presented by Cao *et al.* (2006) and wrote MATLAB® programmes that were used to plot graphs of the kinematical quantities that described the motion of the single toggle jaw crusher.

In this presentation, a convenient, rather unusual, right-handed Cartesian coordinate reference frame (Kalnins, 2009; Mathcentre, 2009; MIT, 2013) is used in setting up a unique kinematical model of the single toggle jaw crusher. The vector loop closure method (Erdman and Sandor, 1991; Kimbrell, 1991; Shigley and Uicker, 1980) is then applied to obtain the kinematical equations in a logical and efficacious manner. This method of kinematical analysis is not in itself new, but, to the authors' knowledge, it has not been used before in the study of jaw crusher mechanics.

Methodology

The analysis presented here is somewhat similar to the works of Cao *et al.* (2006), Deepak (2010) and Garnaik (2010). However, a different formulation of the problem and a different procedure for its solution are used. The resulting derivation of the kinematical equations is rigorous, logical and should be relatively easy to follow.

Generally speaking, the aim of any kinematical analysis of a mechanism is to determine the output motion, given the input motion and the kinematical parameters of the mechanism. In the single toggle jaw crusher mechanism, the input motion is the rotation of the eccentric shaft; the kinematical parameters of the mechanism are the effective lengths of the links that comprise the mechanism; and the output motion is the resulting motion of the swing jaw.

The methods of kinematical analysis can be classified into three categories, namely, graphical, analytical and computer-aided methods. Graphical methods can be likened to still photography because they can deal with only one phase of motion at a time. Moreover, even for a given phase of motion, separate graphical constructions must be done for each of the displacement, velocity and acceleration analyses. Thus, a very large number of graphical constructions would be required to obtain anything close to a complete kinematical description of the mechanism. However, the availability of graphical software has made it easier to use graphical methods.

Analytical methods usually result in a small number of equations that contain all the information that is required to completely describe the kinematics of the mechanism. With these equations, the effects of design alterations can be readily investigated. Therefore, analytical methods are inherently more efficient and powerful, as compared

to graphical methods. Moreover, analytical methods usually are more accurate than graphical methods.

Computer-aided methods use software packages that are specially designed for the purpose. Today, there are many, commercially available, interactive and user-friendly software packages that can be used, not only to simulate the motion of mechanisms but also to determine such quantities as displacements, velocities, accelerations, forces and moments, among others. However, the required software and hardware are expensive, and the user requires a good knowledge of the mechanical principles that govern the behaviour of mechanisms, as well as the skill required to use the software (Monkova *et al.*, 2011). In the design of complex mechanisms, computer-aided methods may be the best choice, but in this study, the mechanism to be analysed is relatively simple, and an analytical method will suffice.

All points in the crushing mechanism of the single toggle jaw crusher are constrained to move in parallel planes. Moreover, the mechanism consists of four links, namely, the eccentric, the swing jaw, the toggle link and the frame, in the form of a closed kinematic chain. All joints in the mechanism are revolute joints. Thus, the mechanism can be modelled as a planar four-bar mechanism with four revolute joints. Further, the analysis of the mechanism recognizes the following two constraints:

(1) All the links in the mechanism are assumed to be completely rigid. Therefore, the effective lengths of the links remain invariant throughout the cycle of motion of the mechanism.

(2) The kinematic chain that constitutes the mechanism remains closed throughout the cycle of motion of the mechanism.

As a result of the above-mentioned constraints, for any phase of motion of the mechanism, the effective lengths of the links can be taken to be vectors, of known magnitudes, that form a closed loop. Consequently, a vector loop closure equation can be written for the mechanism. Beyond this, the analysis of the mechanism is reduced to mathematical routine.

In this paper, starting with a suitable choice of a coordinate reference frame, a kinematical model of the single toggle jaw crusher is established, and then, a kinematical analysis of the model, based on the vector loop closure method (Erdman and Sandor, 1991; Kimbrell, 1991; Shigley and Uicker, 1980) is presented. Application of the results of the kinematical analysis is demonstrated using the dimensional data of a practical single toggle jaw crusher.

The equations obtained in this study should facilitate further studies into aspects of the mechanics of the single toggle jaw crusher, such as static and dynamic force analyses, an understanding of which is essential for sound design of the crusher.

Kinematical model

The concept of the single toggle jaw crusher is illustrated in Figure 1. The swing jaw drive mechanism, which includes the eccentric shaft, the frame, the swing jaw and the toggle link, can be modelled as a planar four bar mechanism that is known as the crank and rocker (Erdman and Sandor, 1991; Kimbrell, 1991).

In the kinematical model, which is illustrated in Figure 2, the eccentric shaft is modelled as a short crank O_2O_3, of length r_2, that continuously rotates about a fixed axis, at O_2. The swing jaw is modelled as the coupler link O_3O_4, of length r_3, which moves with

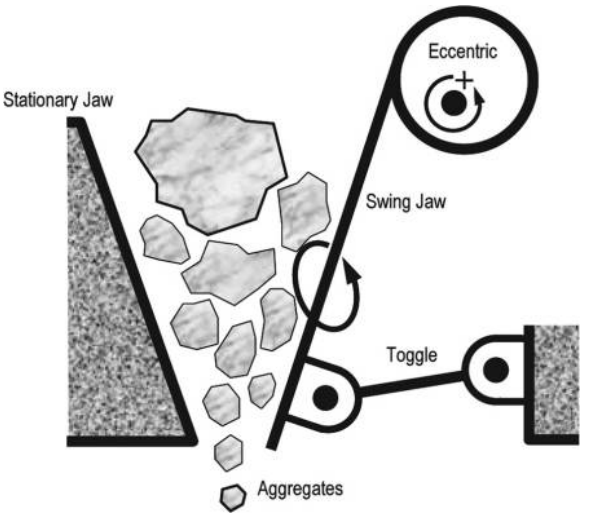

Figure 1.
Concept of the single toggle jaw crusher

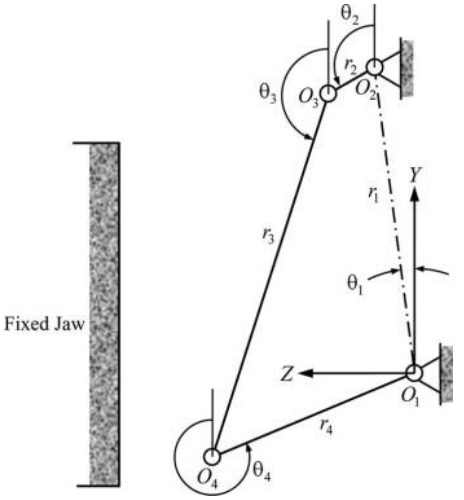

Figure 2.
Kinematical model of the single toggle jaw crusher

a complex planar motion that has both rotational and translational components. The toggle link is modelled as the rocker O_4O_1, which oscillates about the fixed axis at O_1. The fixed jaw is considered to be an integral part of the frame of the machine.

In studying the kinematics of the single toggle jaw crusher, it is particularly important to understand the motion of the coupler link O_3O_4, relative to the fixed jaw, as the crank rotates through a complete cycle. A right-handed Cartesian reference frame that is convenient for analysing this motion will be used, as shown in Figure 2. The X-axis is perpendicular to the plane of the figure, and it points at the reader. Angular displacements are taken counter-clockwise, relative to the positive Y direction.

Kinematical analysis

Vector loop closure

The analysis of position and displacement can be accomplished through the use of the well-known vector loop closure method (Erdman and Sandor, 1991; Kimbrell, 1991; Shigley and Uicker, 1980), which is illustrated in Figure 3.

The vector loop closure equation can be written as follows:

$$\mathbf{r}_1 + \mathbf{r}_2 + \mathbf{r}_3 + \mathbf{r}_4 = 0 \tag{1}$$

Equation (1) can be re-written in the complex vector notation as follows:

$$r_1 e^{j\theta_1} + r_2 e^{j\theta_2} + r_3 e^{j\theta_3} + r_4 e^{j\theta_4} = 0 \tag{2}$$

Moreover, the Euler identities state as follows (Carmichael and Smith, 1962):

$$\left.\begin{aligned} e^{j\theta} &= \cos\theta + j\sin\theta \\ e^{-j\theta} &= \cos\theta - j\sin\theta \end{aligned}\right\} \tag{3}$$

For conciseness, let us introduce the following notation:

$$\left.\begin{aligned} \cos\theta_i &= c_i \\ \sin\theta_i &= s_i \end{aligned}\right\} \tag{4}$$

By using equations (3) and (4), equation (2) may be re-written as follows:

$$r_1(c_1 + js_1) + r_2(c_2 + js_2) + r_3(c_3 + js_3) + r_4(c_4 + js_4) = 0 \tag{5}$$

In equation (5), if the real terms and the imaginary terms are considered separately, the following two equations are readily obtained:

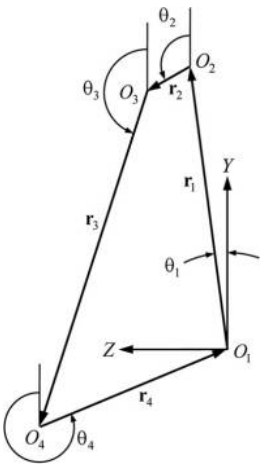

Figure 3.
Vector loop closure diagram

$$\left.\begin{aligned} r_1c_1 + r_2c_2 &= -(r_3c_3 + r_4c_4) \\ r_1s_1 + r_2s_2 &= -(r_3s_3 + r_4s_4) \end{aligned}\right\} \tag{6}$$

By squaring each of equations (6), the following is obtained:

$$\left.\begin{aligned} r_1^2c_1^2 + 2r_1r_2c_1c_2 + r_2^2c_2^2 &= r_3c_3^2 + 2r_3r_4c_3c_4 + r_4^2c_4^2 \\ r_1^2s_1^2 + 2r_1r_2s_1s_2 + r_2^2s_2^2 &= r_3s_3^2 + 2r_3r_4s_3s_4 + r_4^2s_4^2 \end{aligned}\right\} \tag{7}$$

By adding corresponding terms in equations (7), and noting that $c_i^2 + s_i^2 = 1$, the following is obtained:

$$r_1^2 + 2r_1r_2c_1c_2 + 2r_1r_2s_1s_2 + r_2^2 = r_3^2 + 2r_4c_4(r_3c_3) + 2r_4s_4(r_3s_3) + r_4^2 \tag{8}$$

Now, equations (6) can be rearranged into the following:

$$\left.\begin{aligned} r_3c_3 &= -(r_1c_1 + r_2c_2 + r_4c_4) \\ r_3s_3 &= -(r_1s_1 + r_2s_2 + r_4s_4) \end{aligned}\right\} \tag{9}$$

Moreover, it is known from trigonometry that (Carmichael and Smith, 1962):

$$\cos\theta_i\cos\theta_k + \sin\theta_i\sin\theta_k = \cos(\theta_i - \theta_k) \tag{10}$$

By substituting equation (9) into equation (8), and using the identity in equation (10), the following is obtained:

$$\left.\begin{aligned} 2r_1r_2\cos(\theta_2 - \theta_1) + 2r_1r_4\cos(\theta_4 - \theta_1) + 2r_2r_4\cos(\theta_4 - \theta_2) \\ = r_3^2 - r_1^2 - r_2^2 - r_4^2 \end{aligned}\right\} \tag{11}$$

In Figure 2, θ_1 is a fixed quantity. Moreover, the motion of the crank O_2O_3 is the input motion and may be considered to be a rotation at uniform angular velocity, ω_2. Thus, at an instant in time, t, after commencement of the motion, the value of θ_2, in radians, will be determined as follows:

$$\theta_2(t) = \omega_2 t \tag{12}$$

For given values of r_1, r_2, r_3, r_4 and θ_1, equation (11) can be used to determine the value of θ_4 that corresponds to any given value of θ_2. In that case, equation (11) will, therefore, describe all the possible phases of motion of the mechanism.

Freudenstein's equation

In the special case where $\theta_1 = 0$, equation (11) reduces to the following:

$$2r_1r_2\cos\theta_2 + 2r_1r_4\cos\theta_4 + 2r_2r_4\cos(\theta_4 - \theta_2) = r_3^2 - r_1^2 - r_2^2 - r_4^2 \tag{13}$$

Each of the terms in equation (13) can be divided by $2r_2r_4$, and the resulting equation can be re-arranged to obtain the following:

$$\frac{r_1}{r_4}\cos\theta_2 + \frac{r_1}{r_2}\cos\theta_4 + \frac{r_1^2 + r_2^2 + r_4^2 - r_3^2}{2r_2r_4} = \cos(\theta_4 - \theta_2) \tag{14}$$

Equation (14) can be re-written as follows:

$$\left.\begin{aligned} K_1\cos\theta_2 + K_2\cos\theta_4 + K_3 &= \cos(\theta_4 - \theta_2) \\ K_1 &= \frac{r_1}{r_4} \\ K_2 &= \frac{r_1}{r_2} \\ K_3 &= \frac{r_1^2 + r_2^2 - r_3^2 + r_4^2}{2r_2r_4} \end{aligned}\right\} \tag{15}$$

Equation (15) is the well-known Freudenstein's equation that has been commonly used in the synthesis of four bar mechanisms (Erdman and Sandor, 1991; Kimbrell, 1991; Shigley and Uicker, 1980).

Angular displacement of the swing jaw

In the study and design of the single toggle jaw crusher, the motion of the coupler (swing jaw) is of greater interest than that of the rocker (toggle link).

Let us now rearrange equation (6) into the following:

$$\left.\begin{aligned} r_1c_1 + r_2c_2 + r_3c_3 &= -r_4c_4 \\ r_1s_1 + r_2s_2 + r_3s_3 &= -r_4s_4 \end{aligned}\right\} \tag{16}$$

By substituting equation (16) into equation (8) and using equation (10), the following is obtained:

$$\left.\begin{aligned} 2r_1r_2\cos(\theta_2 - \theta_1) + 2r_2r_3\cos(\theta_3 - \theta_2) + 2r_3r_1\cos(\theta_3 - \theta_1) \\ = r_4^2 - r_3^2 - r_2^2 - r_1^2 \end{aligned}\right\} \tag{17}$$

For given lengths of the four links in the mechanism, along with the value of θ_1, equation (17) can be used to determine corresponding values of θ_3 for given values of θ_2. When compared to equation (11), equation (17) is of greater utility in describing the motion of the swing jaw, relative to that of the crank.

If $\theta_1 = 0$, equation (17) reduces to the following:

$$2r_1r_2\cos\theta_2 + 2r_3r_1\cos\theta_3 + r_4^2 - r_3^2 - r_2^2 - r_1^2 = -2r_2r_3\cos(\theta_3 - \theta_2) \tag{18}$$

Equation (18) can be divided through by $2r_2r_3$ to obtain the following:

$$\frac{r_1}{r_3}\cos\theta_2 + \frac{r_1}{r_2}\cos\theta_3 + \frac{r_4^2 - r_3^2 - r_2^2 - r_1^2}{2r_2r_3} = -\cos(\theta_3 - \theta_2) \tag{19}$$

Equation (19) can be re-written as follows:

$$\left.\begin{aligned} K_1 \cos\theta_2 + K_2 \cos\theta_3 + K_3 &= -\cos(\theta_3 - \theta_2) \\ K_1 &= \frac{r_1}{r_3} \\ K_2 &= \frac{r_1}{r_2} \\ K_3 &= \frac{r_4^2 - r_3^2 - r_2^2 - r_1^2}{2r_2 r_3} \end{aligned}\right\} \quad (20)$$

Equation (20) may be regarded as another version of Freudenstein's equation. For given values of the lengths of the four links, the equation can be used to determine the values of θ_3 that correspond to given values of θ_2.

Position and displacement of a point in the swing jaw

It should be informative to determine the motion of a given point in the swing jaw, relative to the motion of the crank, especially for those points that fall on the crushing surface of the swing jaw. For the purpose of locating such points, the coordinate system illustrated in Figure 4 will be used.

In Figure 4, the $Y'Z'$ coordinate reference frame has its origin at O_3, and it is fixed in the swing jaw. The point P too is fixed in the swing jaw, and its position is located by the vector $\mathbf{r}_5$, of magnitude r_5, whose origin is at O_3 and whose direction is indicated by the angle ϕ_5. Thus:

$$\left.\begin{aligned} y' &= r_5 \cos\phi_5 \\ z' &= r_5 \sin\phi_5 \end{aligned}\right\} \quad (21)$$

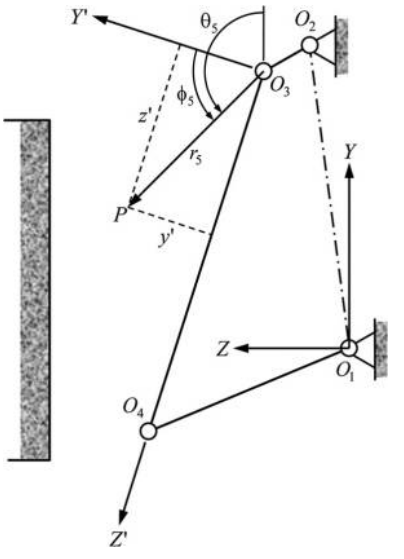

Figure 4.
Location of a point P in the swing jaw

The direction of the vector $\mathbf{r}_5$ taken relative to the Y direction is indicated by the angle θ_5, such that:

$$\theta_5 = (\theta_3 + \phi_5 - 90)^0 \tag{22}$$

Thus:

$$\left.\begin{aligned} \sin\theta_5 &= -\cos(\theta_3 + \phi_5) = \sin\theta_3 \sin\phi_5 - \cos\theta_3 \cos\phi_5 \\ \cos\theta_5 &= \sin(\theta_3 + \phi_5) = \sin\theta_3 \cos\phi_5 + \cos\theta_3 \sin\phi_5 \end{aligned}\right\} \tag{23}$$

In the special case, where $\phi_5 = 90^0$, θ_5 becomes equal to θ_3 and the point P then lies on the line O_3O_4, at a distance of r_5 from O_3.

In Figure 4, the location of point P relative to the YZ coordinate reference frame may now be expressed as follows:

$$\left.\begin{aligned} y_P &= r_1 \cos\theta_1 + r_2 \cos\theta_2 + r_5 \cos\theta_5 \\ z_P &= r_1 \sin\theta_1 + r_2 \sin\theta_2 + r_5 \sin\theta_5 \end{aligned}\right\} \tag{24}$$

By using equation (23), equation (24) can be re-written as follows:

$$\left.\begin{aligned} y_P &= r_1 \cos\theta_1 + r_2 \cos\theta_2 + r_5(\sin\theta_3 \cos\phi_5 + \cos\theta_3 \sin\phi_5) \\ z_P &= r_1 \sin\theta_1 + r_2 \sin\theta_2 + r_5(\sin\theta_3 \sin\phi_5 - \cos\theta_3 \cos\phi_5) \end{aligned}\right\} \tag{25}$$

In the special case where $\phi_5 = 90^0$, equation (25) reduces to the following:

$$\left.\begin{aligned} y_P &= r_1 \cos\theta_1 + r_2 \cos\theta_2 + r_5 \cos\theta_3 \\ z_P &= r_1 \sin\theta_1 + r_2 \sin\theta_2 + r_5 \sin\theta_3 \end{aligned}\right\} \tag{26}$$

Given the lengths r_1, r_2, r_3 and r_4 of the links, along with the angle θ_1, equations (17) and (26) can be used to determine the *locus* of any point on the line O_3O_4, for a complete cycle of rotation of the crank O_2O_3, provided that the distance r_5 of that point from O_3 is known.

Angular velocity of the swing jaw

An expression for the angular velocity of the coupler (swing jaw) can be obtained by differentiating equation (17) with respect to time. In doing so, it should be borne in mind that r_1, θ_1, r_2, r_3 and r_4 are all constants with respect to time. The result of the differentiation is then as follows:

$$\left.\begin{aligned} r_1 r_2 \sin(\theta_2 - \theta_1)\frac{d\theta_2}{dt} + r_2 r_3 \sin(\theta_3 - \theta_2)\frac{d\theta_3}{dt} + r_3 r_1 \sin(\theta_3 - \theta_1)\frac{d\theta_3}{dt} \\ = r_2 r_3 \sin(\theta_3 - \theta_2)\frac{d\theta_2}{dt} \end{aligned}\right\} \tag{27}$$

Equation (27) can be divided through by $r_2 r_3$ to obtain the following:

$$\left.\begin{aligned} \frac{r_1}{r_3}\sin(\theta_2 - \theta_1)\frac{d\theta_2}{dt} + \sin(\theta_3 - \theta_2)\frac{d\theta_3}{dt} + \frac{r_1}{r_2}\sin(\theta_3 - \theta_1)\frac{d\theta_3}{dt} \\ = \sin(\theta_3 - \theta_2)\frac{d\theta_2}{dt} \end{aligned}\right\} \tag{28}$$

Moreover, the following additional notation can be introduced:

$$\frac{d\theta_2}{dt} = \omega_2; \quad \frac{d\theta_3}{dt} = \omega_3 \tag{29}$$

Velocity of a point in the swing jaw

The position of a point in the swing jaw is determined by equation (25). In the particular case where the point falls on line O_3O_4, its position is then described by equation (26). Thus, the vertical and horizontal components of the velocity of a point on line O_3O_4 can be determined by differentiating equation (26) with respect to time, to obtain the following:

$$\left.\begin{aligned} v_{PV} = \dot{y}_P = -\omega_2 r_2 \sin\theta_2 - \omega_3 r_5 \sin\theta_3 \\ v_{PH} = \dot{z}_P = \omega_2 r_2 \cos\theta_2 + \omega_3 r_5 \cos\theta_3 \end{aligned}\right\} \tag{30}$$

Angular acceleration of the swing jaw

An expression for the angular acceleration of the coupler can be obtained by differentiating equation (27) with respect to time. In doing so, it should be borne in mind that r_1, θ_1, r_2, r_3, r_4 and ω_2 are all constants with respect to time. The result of the differentiation is then as follows:

$$\left.\begin{aligned} r_1 r_2 \omega_2^2 \cos(\theta_2 - \theta_1) + r_2 r_3 \omega_3(\omega_3 - \omega_2)\cos(\theta_3 - \theta_2) \\ + r_2 r_3 \sin(\theta_3 - \theta_2)\frac{d\omega_3}{dt} + r_3 r_1 \omega_3^2 \cos(\theta_3 - \theta_1) \\ + r_3 r_1 \sin(\theta_3 - \theta_1)\frac{d\omega_3}{dt} \\ = r_2 r_3 \omega_2(\omega_3 - \omega_2)\cos(\theta_3 - \theta_2) \end{aligned}\right\} \tag{31}$$

Here, the following additional notation can be introduced:

$$\frac{d\omega_3}{dt} = \alpha_3 \tag{32}$$

With the use of equation (32), equation (31) can now be re-arranged into the following:

$$\left.\begin{aligned} r_1 r_2 \omega_2^2 \cos(\theta_2 - \theta_1) + r_2 r_3(\omega_3 - \omega_2)^2 \cos(\theta_3 - \theta_2) \\ + r_3 r_1 \omega_3^2 \cos(\theta_3 - \theta_1) \\ = -[r_2 r_3 \sin(\theta_3 - \theta_2) + r_3 r_1 \sin(\theta_3 - \theta_1)]\alpha_3 \end{aligned}\right\} \tag{33}$$

Equation (33) can be divided through by $r_2 r_3$ to obtain the following:

$$\left.\begin{aligned}\frac{r_1}{r_3}\omega_2{}^2\cos(\theta_2-\theta_1)+(\omega_3-\omega_2)^2\cos(\theta_3-\theta_2)+\frac{r_1}{r_2}\omega_3{}^2\cos(\theta_3-\theta_1)\\ =-\left[\sin(\theta_3-\theta_2)+\frac{r_1}{r_2}\sin(\theta_3-\theta_1)\right]\alpha_3\end{aligned}\right\} \quad (34)$$

Acceleration of a point in the swing jaw

The vertical and horizontal components of the acceleration of a point on line O_3O_4 can be determined by differentiating equation (30) with respect to time, to obtain the following:

$$\left.\begin{aligned}a_{PV}=\ddot{y}_P=-\omega_2{}^2r_2\cos\theta_2-\omega_3{}^2r_5\cos\theta_3-\alpha_3r_5\sin\theta_3\\ a_{PH}=\ddot{z}_P=-\omega_2{}^2r_2\sin\theta_2-\omega_3{}^2r_5\sin\theta_3+\alpha_3r_5\cos\theta_3\end{aligned}\right\} \quad (35)$$

In equation (35), if r_5 is given, then, for any given value of θ_2, the corresponding values of θ_3, ω_3 and α_3 can be determined, and therefore, the acceleration components a_{PV} and a_{PH} can also be determined.

Application and discussion of the results of the Kinematical analysis

Cao *et al.* (2006) used the dimensional data for a PE 400 × 600 single toggle jaw crusher, as shown in Table I.

From the data in Table I, it follows, to good approximation, that $r_1 = 817$ mm and $\theta_1 = 3.18^0$. We shall adopt these data, as we proceed in this paper.

Determination of the angular displacement of the swing jaw

By using the above-mentioned data, equation (17) can be reduced to the following:

$$\left.\begin{aligned}K_1\cos\theta_3+K_2\sin\theta_3+K_3=0\\ K_1=\cos\theta_2+68\\ K_2=\sin\theta_2+3.8\\ K_3=62.9+0.752\cos\theta_2+0.042\sin\theta_2\end{aligned}\right\} \quad (36)$$

In equation (36), for any given value of θ_2, K_1, K_2 and K_3 can be determined. Moreover, the first of equation (36) may be re-written as follows:

$$K_1\cos\theta_3=-(K_2\sin\theta_3+K_3) \quad (37)$$

By squaring both sides of equation (37), using the well-known trigonometric identity, $\cos^2\theta = 1-\sin^2\theta$, and then re-arranging the result, the following can be obtained:

Table I.
Data for a PE 400 × 600 single toggle jaw crusher (mm)

$r_1\sin\theta_1$	$r_1\cos\theta_1$	r_2	r_3	r_4
45.3	815.7	12	1,085	455

$$\left.\begin{aligned} A\sin^2\theta_3 + B\sin\theta_3 + C = 0 \\ A = K_2^2 + K_1^2 \\ B = 2K_2K_3 \\ C = K_3^2 - K_1^2 \end{aligned}\right\} \quad (38)$$

Equation (38) is a quadratic in sin θ_3, and it can, therefore, be solved to yield two values of θ_3. Thus, there are two possible configurations of the four bar mechanism illustrated in Figure 2 for every given value of θ_2. However, only one of these configurations will be suitable for the proper functioning of the crusher mechanism. The suitable configuration should have the values of θ_3 falling between 90^0 and 180^0. The unsuitable configuration would have values of θ_3 that are greater than 180^0, as shown in Figure 5.

For the suitable configuration of the mechanism, as shown in Figure 2, equations (36) and (38) were used in a Microsoft Excel® Worksheet, along with the data in Table I, to determine the values of θ_3, as θ_2 was varied from 0^0 to 360^0. Some of these calculated values are given in Table II. For one full cycle of rotation of the crank, the minimum value of θ_3 was found to be 159.7^0, whereas the maximum value of θ_3 was found to be

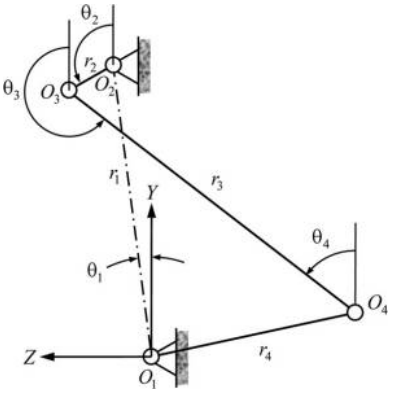

Figure 5.
Another possible configuration of the mechanism

θ_2 (degrees)	θ_3 (degrees)	θ_2 (degrees)	θ_3 (degrees)
0	160.2	195	160.8
15	160.5	210	160.6
30	160.7	225	160.4
45	160.9	240	160.1
60	161.1	255	160
75	161.3	270	159.8
90	161.5	285	159.7
105	161.5	300	159.7
120	161.6	315	159.8
135	161.5	330	159.9
150	161.4	345	160
165	161.3	360	160.2
180	161.1		

Table II.
Analytically determined values of θ_3 for given values of θ_2

161.6^0. Thus, the range of variation of θ_3 is less than 2^0. The change in angular orientation of the swing jaw, during its cycle of motion, is quite small.

During the cycle of motion of the mechanism, two particular phases are of special interest. These special phases, which are known as toggle positions (Shigley and Uicker, 1980), occur when the crank O_2O_3 and the coupler O_3O_4 fall on the same straight line. For this to happen, either θ_3 must be equal to $(\theta_2 + 180)$ degrees or θ_3 must be equal to θ_2. When these conditions are used in equation (17), along with the data in Table I, it is found that the toggle positions will occur when $\theta_2 = 161.35$ and when $\theta_2 = 340^0$. In determining the toggle positions, due regard must be given to the fact that, for each value of θ_2, there will be two possible configurations of the mechanism, only one of which will be suitable for the proper operation of the crusher.

A graph of the variation of θ_3 with θ_2 is shown in Figure 6.

For a given set of the values of θ_1, θ_2 and θ_3, along with knowledge of the lengths of the four links in the mechanism, the corresponding values of θ_4 can be readily determined using equation (16).

Determination of the position and displacement of a point in the swing jaw

Five points were selected along the length of the line O_3O_4, whose distances from O_3 are given in Table III. The point $P1$ is coincident with O_3, and the point $P5$ is coincident with O_4. The rest of the points are uniformly spaced along the length of the line O_3O_4.

Using equation (26), along with the data given in Tables I and III, the positions of the points $P1$ through to $P5$ were determined for one complete cycle of motion of the mechanism. The data in Tables IV and V are representative of the results.

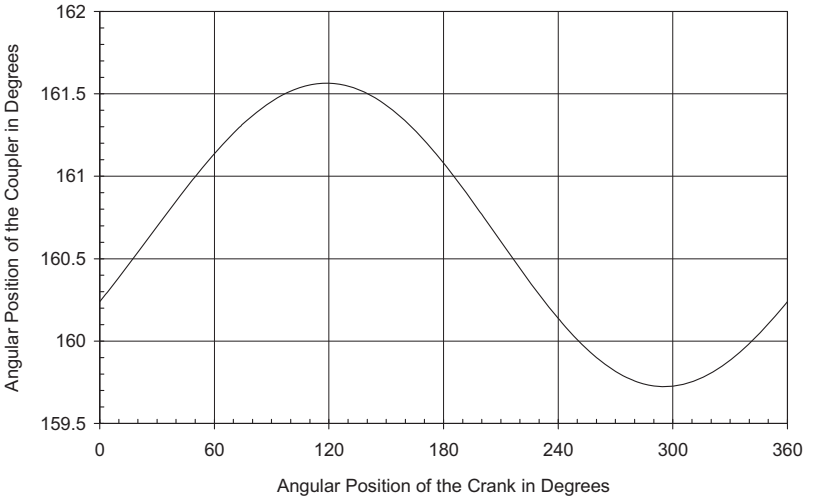

Figure 6.
Variation of coupler angle θ_3 with crank angle θ_2

Table III.
Locations of selected points along the coupler

Point	$P1$	$P2$	$P3$	$P4$	$P5$
r_5 (mm)	0	271.25	542.5	813.75	1,085

As can be seen in Table IV, the range of displacement in the Y direction increases monotonously, and at a slightly increasing rate, as we move from point $P1$ through to $P5$. Motion of the swing jaw in the Y direction causes a rubbing action between the material being crushed and the swing jaw, thereby causing the crushing surface of the swing jaw to wear. One could, therefore, expect an increasing wear rate as we move from $P1$ through to $P5$. On the other hand, during the crushing stroke, any motion of the swing jaw in the downward vertical direction forcefully feeds the material being crushed into the crushing chamber, which is desirable because it increases the throughput of the crusher.

In Table V, the range of displacement in the Z direction decreases at a decreasing rate, as we move from point $P1$ through to $P4$ but then increases as we move from point $P4$ to $P5$. Displacement of the swing jaw in the Z direction should be the greater contributor to the crushing action.

The loci of points $P1$ through to $P5$, for one complete cycle of motion, are shown in Figures 7-11. These loci have been referred to as coupler curves (Kimbrell, 1991; Martin George, 1982; Shigley and Uicker, 1980).

In Figures 7-11, the scales on the Y and the Z axes should be equal for the forms of the loci to be correct. In Figure 7, the *locus* of point $P1$ is the circle that is described by the crankpin O_3 and centred at O_2. With the data that were used to determine these loci, this circle has a radius of 12 mm.

As can be seen in Figures 8, 9 and 10, the loci of points $P2$, $P3$ and $P4$ appear to be ellipses of varying proportions. As we move from point $P2$ to $P3$ and on to $P4$, the major axis of the ellipses grows longer, whereas the minor axis grows shorter. Moreover, the major and minor axes of these ellipses are increasingly angled relative to the YZ coordinate reference frame.

In Figure 11, the *locus* of point $P5$ is in reality a circular arc that is described by the rocker pin O_4 and centred at O_1. With the data that were used to determine the loci, the rocker has a length of 455 mm, and the rocker pin O_4 would describe a circle of circumference 2,859 mm in one complete rotation. However, for one complete rotation of the crank, the range of oscillation of the rocker is only 4.39^0. Thus, the length of the arc described by the rocker pin O_4 is only about 35 mm or 1.2 per cent of the circumference of the complete circle. Therefore, the arc described by the rocker pin O_4 is infinitesimal compared to the complete circle that it is a part of. This is why its curvature is hardly noticeable in Figure 11.

Table IV. Ranges of displacements in the Y direction

Point	$P1$	$P2$	$P3$	$P4$	$P5$
y_{min} (mm)	803.75	547.09	290.32	33.46	−223.47
y_{max} (mm)	827.75	572.54	317.45	62.46	−192.44
Range of y	24	25.45	27.13	29	31.03

Table V. Ranges of displacements in the Z direction

Point	$P1$	$P2$	$P3$	$P4$	$P5$
z_{min} (mm)	33.18	126.57	219.02	308.98	396.52
z_{max} (mm)	57.18	143.67	231.02	320.44	412.44
Range of z	24	17.10	12.00	11.46	15.92

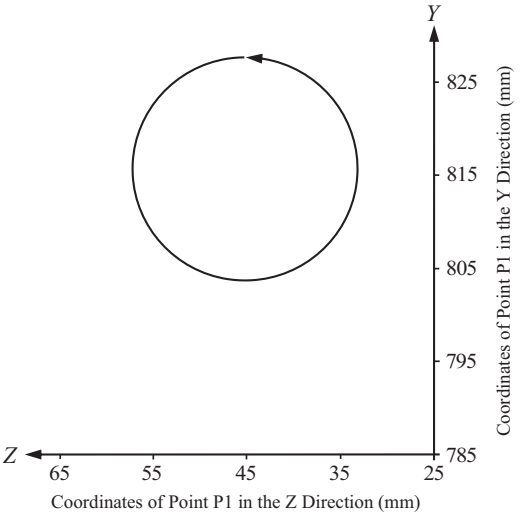

Figure 7.
The *Locus* of point P1 for one complete cycle of motion

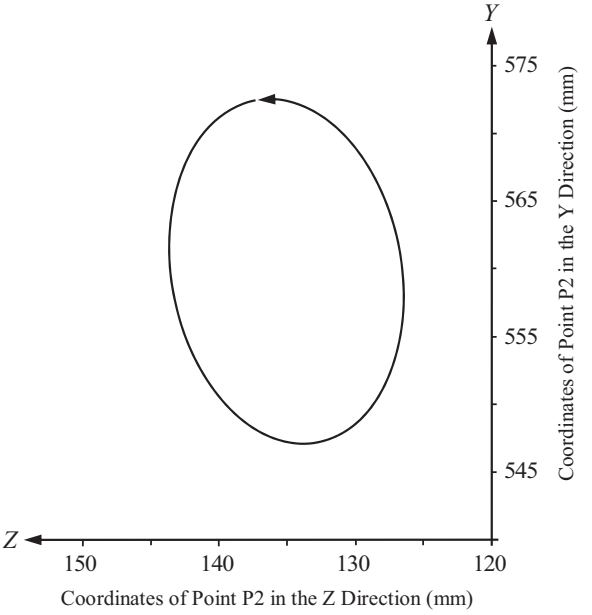

Figure 8.
The *Locus* of point P2 for one complete cycle of motion

Determination of the angular velocity of the swing jaw

Although ω_3 is expected to vary with time, the crank (eccentric shaft) is assumed to rotate at constant rotational velocity, and therefore, ω_2 should be constant. According to a manufacturer's specifications (Henan Hongxing Mining Machinery Company Limited, 2013), for a PE 400 × 600 single toggle jaw crusher, ω_2 may be taken to be 275 rpm or

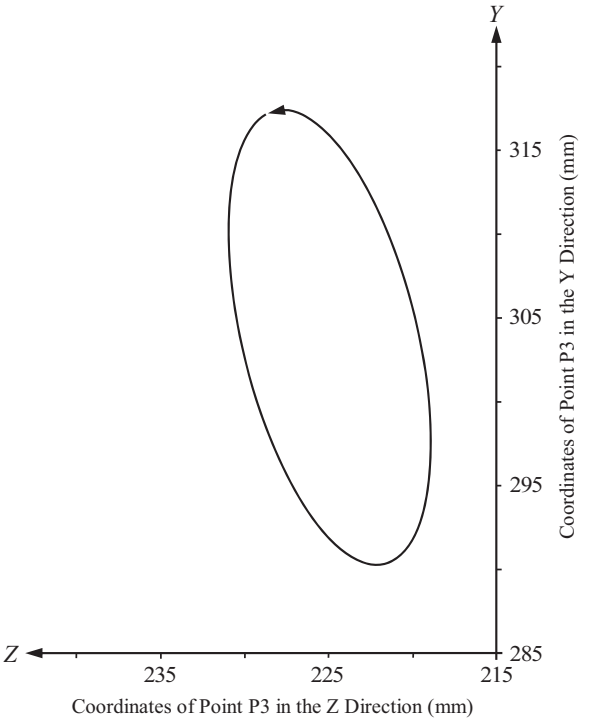

Figure 9.
The *Locus* of point P3 for one complete cycle of motion

28.8 radians per second. Thus, with the data given in Table I, equation (28) may be re-written as follows:

$$\left.\begin{aligned} \omega_3 &= \left(\frac{K_2 - K_1}{K_2 + K_3}\right)\omega_2 = 28.8\left(\frac{K_2 - K_1}{K_2 + K_3}\right) \\ K_1 &= \frac{r_1}{r_3}\sin(\theta_2 - \theta_1) = 0.753\sin(\theta_2 - \theta_1) \\ K_2 &= \sin(\theta_3 - \theta_2) \\ K_3 &= \frac{r_1}{r_2}\sin(\theta_3 - \theta_1) = 68.08\sin(\theta_3 - \theta_1) \end{aligned}\right\} \quad (39)$$

In equation (39), for any given value of θ_2, with the corresponding value of θ_3 having been determined, K_1, K_2 and K_3 can be determined.

Equation (39) was used to determine the values of ω_3, as θ_2 was varied from 0^0 to 360^0. Some of the calculated values are given in Table VI.

For one full cycle of rotation of the crank, the minimum value of ω_3 was found to be -0.476 radians per second or -4.55 rpm, whereas the maximum value of ω_3 was found to be 0.451 radians per second or 4.3 rpm. Thus, the angular velocity of the coupler (swing jaw) is generally small.

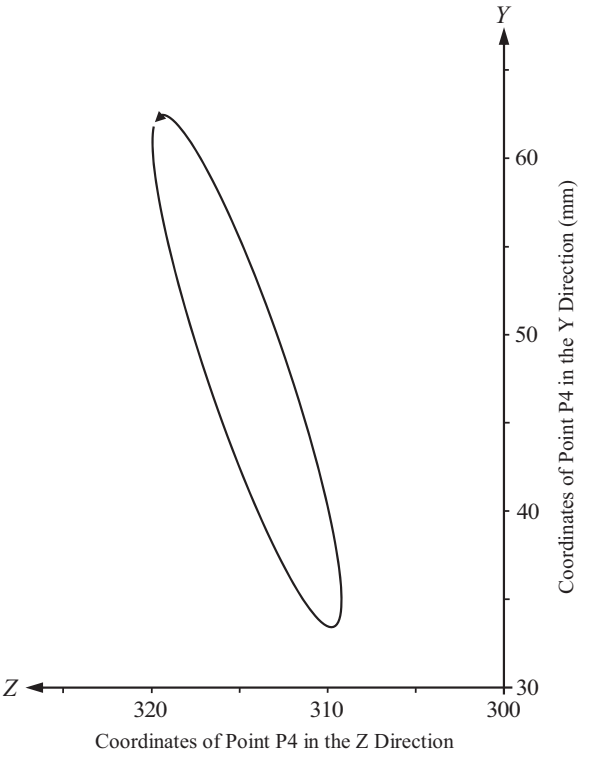

Figure 10.
The *Locus* of point P4 for one complete cycle of motion

A graph of the variation of ω_3 with θ_2 is shown in Figure 12. Note in Figure 12 that the angular velocity of the swing jaw becomes zero at the instances where the angular displacement of the swing jaw attained maximum and minimum values, as can be seen in Figure 6. This is to be expected because it is at these instances that the rate of change of angular displacement of the swing jaw instantaneously becomes zero.

Determination of the velocity of a point in the swing jaw

With the data given in Table I and with the value of ω_2 taken to be 28.8 radians per second, equation (30) can be re-written as follows:

$$\left.\begin{aligned} v_{PV} = \dot{y}_P = & -0.3456 \sin\theta_2 - \omega_3 r_5 \sin\theta_3 \\ v_{PH} = \dot{z}_P = & \ 0.3456 \cos\theta_2 + \omega_3 r_5 \cos\theta_3 \end{aligned}\right\} \tag{40}$$

In equation (40), if r_5 is given, in metres, then, for any given value of θ_2, the corresponding values of θ_3 and ω_3 can be determined, as was earlier done, and therefore, the velocity components v_{PV} and v_{PH} can be determined in metres per second.

For the values of r_5 given in Table III, the values of the velocity components v_{PV} and v_{PH} were determined for one complete cycle of motion of the mechanism. The data in Tables VII and VIII are representative of the results.

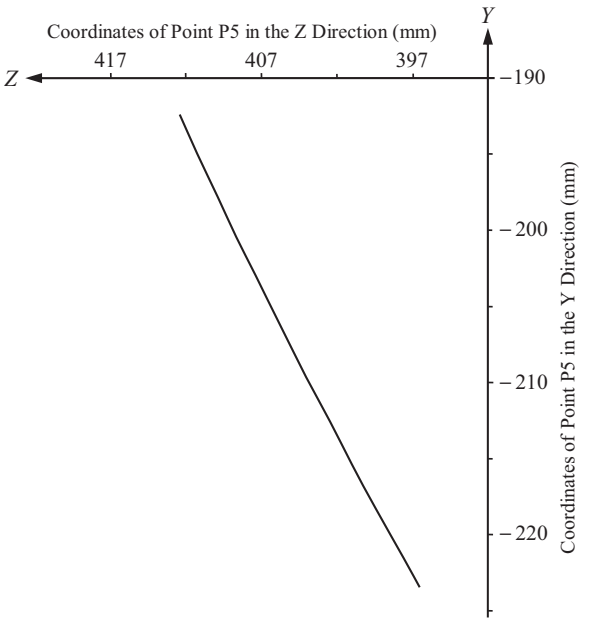

Figure 11.
The *Locus* of point P5 for one complete cycle of motion

θ_2 (degrees)	ω_3 (rad/s)	θ_2 (degrees)	ω_3 (rad/s)
0	0.407	195	−0.463
15	0.443	210	−0.476
30	0.450	225	−0.454
45	0.429	240	−0.397
60	0.381	255	−0.313
75	0.309	270	−0.206
90	0.216	285	−0.087
105	0.108	300	0.036
120	−0.009	315	0.154
135	−0.129	330	0.259
150	−0.242	345	0.345
165	−0.341	360	0.407
180	−0.417		

Table VI.
Analytically determined values of ω_3 for given values of θ_2

In Table VII, negative values of velocity indicate a vertically downward motion, whereas positive values indicate a vertically upward motion. As can be seen in Table VII, the maximum value of the component of velocity in the Y direction, whether it is directed upward or downward, increases monotonously, and at a slightly increasing rate, as we move from point $P1$ through to $P5$. Once again, this could suggest an increasing rate of wear as we move from $P1$ through to $P5$. Moreover, as we move from point $P2$ through to $P5$, slightly greater velocities are achieved in the vertically upward direction, as compared to the vertically downward direction, although the difference is small.

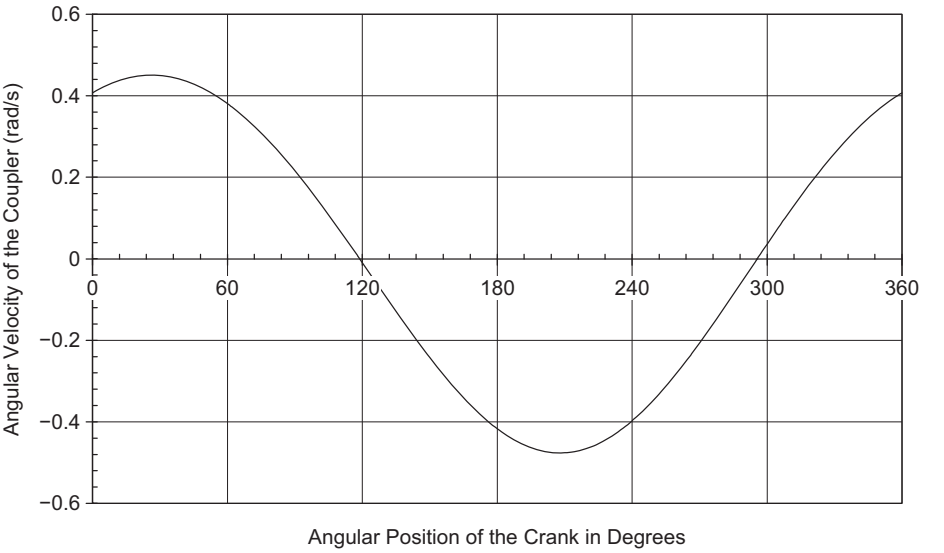

Figure 12.
Variation of coupler angular velocity ω_3 with crank angle θ_2

Table VII.
Velocities in the Y direction

Point	*P*1	*P*2	*P*3	*P*4	*P*5
$\dot{y}_{min}$ (m/s)	−0.346	−0.366	−0.389	−0.414	−0.442
$\dot{y}_{max}$ (m/s)	0.346	0.367	0.393	0.421	0.452

Table VIII.
Velocities in the Z direction

Point	*P*1	*P*2	*P*3	*P*4	*P*5
$\dot{z}_{min}$ (m/s)	−0.346	−0.383	−0.421	−0.46	−0.50
$\dot{z}_{max}$ (m/s)	0.346	0.383	0.421	0.46	0.50

The vertical components of velocity for points *P*1 through to *P*5 are compared graphically in Figure 13, for one complete rotation of the crank. It can be seen in Figure 12 that the angular oscillation of the swing jaw instantaneously stops when $\theta_2 \cong 118.81^0$ and when $\theta_2 \cong 295.625^0$. With no angular oscillation of the swing jaw, its motion becomes a pure translation and all the points in it have the same vertical components of velocity, as can be seen in Figure 13.

In Table VIII, negative values of velocity indicate that the swing jaw is moving away from the fixed jaw, whereas positive values indicate that the swing jaw is moving towards the fixed jaw. As can be seen in Table VIII, the maximum value of the component of velocity in the *Z* direction increases at an almost constant rate, as we move from point *P*1 through to *P*5. Moreover, as we move from point *P*1 through to *P*5, the maximum value of the component of velocity in the *Z* direction appears to remain unchanged, whether the swing jaw is moving towards the fixed jaw or away from the fixed jaw.

The horizontal components of velocity for points *P*1 through to *P*5 are compared graphically in Figure 14, for one complete rotation of the crank. Again, the instances

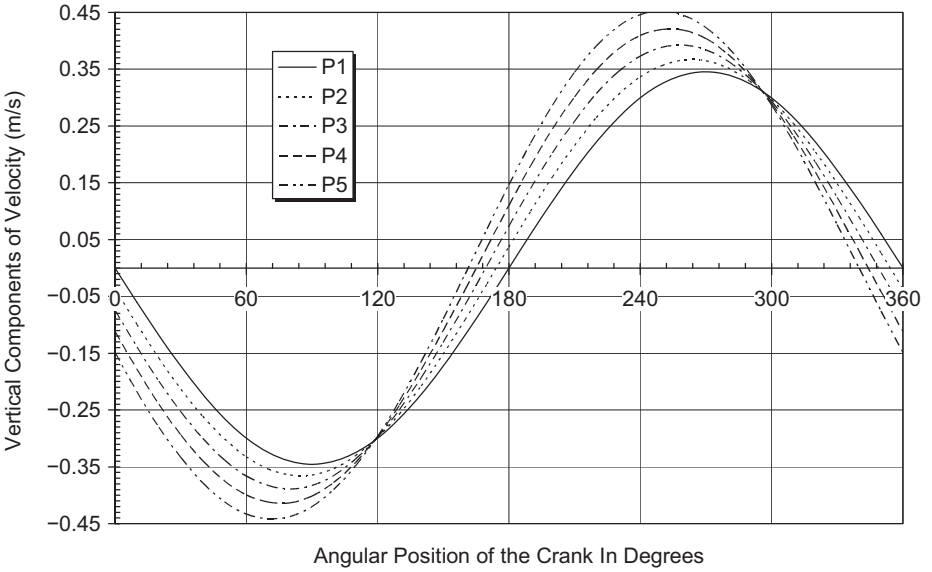

Figure 13. Vertical components of velocity of points in the swing jaw

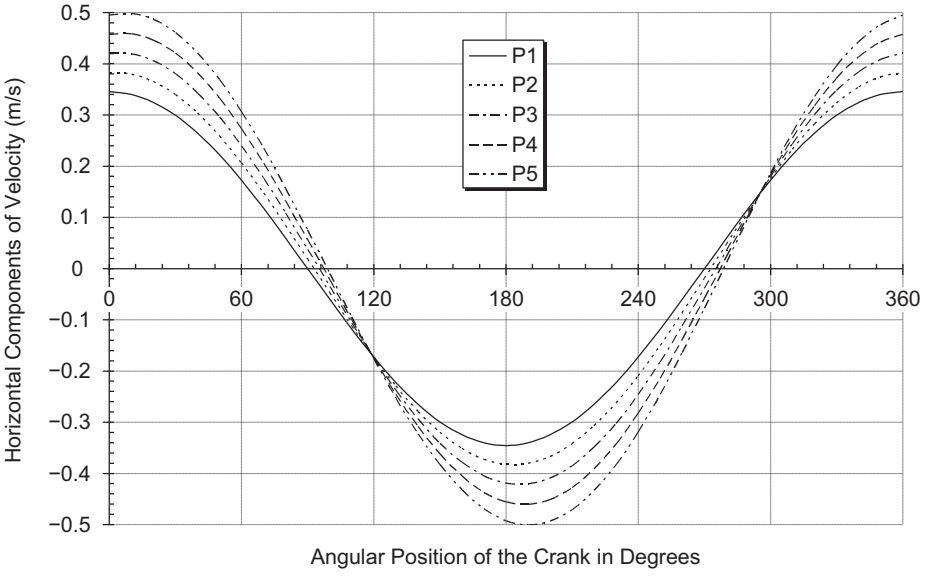

Figure 14. Horizontal components of velocity of points in the swing jaw

when the angular oscillation of the swing jaw instantaneously stops are evidenced in Figure 14 by the crank positions at which all the points in the swing jaw have equal horizontal (as well as vertical) components of velocity.

In Figures 13 and 14, it can be seen that, for approximately the first quarter of rotation of the crank, the swing jaw moves vertically downward and horizontally towards the fixed jaw, thus forcefully feeding the charge of material into the crushing chamber and

simultaneously crushing it. For the second quarter of rotation of the crank, the swing jaw still moves vertically downward but horizontally away from the fixed jaw, thus letting the crushed material fall through the crushing chamber. For the third quarter of rotation of the crank, the swing jaw moves vertically upwards and horizontally away from the fixed jaw, still letting the crushed material fall through the crushing chamber. Finally, in the last quarter of rotation of the crank, the swing jaw continues to move vertically upwards but horizontally towards the fixed jaw, thus beginning another crushing cycle.

Determination of the angular acceleration of the swing jaw

By letting $\omega_2 = 28.8$ radians per second, as was done before, and using the data in Table I, equation (34) may be re-written as follows:

$$\left.\begin{aligned} \alpha_3 &= (K_1 + K_2 + K_3)/K_4 \\ K_1 &= 624.56\cos(\theta_2 - \theta_1) \\ K_2 &= (\omega_3 - 28.8)^2\cos(\theta_3 - \theta_2) \\ K_3 &= 68.08\,\omega_3^2\cos(\theta_3 - \theta_1) \\ K_4 &= -[\sin(\theta_3 - \theta_2) + 68.08\sin(\theta_3 - \theta_1)] \end{aligned}\right\} \quad (41)$$

With the values of θ_3 and ω_3 that correspond to given values of θ_2 having been determined, equation (41) was used to determine the values of α_3 as θ_2 was varied from 0^0 to 360^0. Some of the calculated values are given in Table IX.

For one complete cycle of motion of the swing jaw, the minimum value of its angular acceleration occurred at $\theta_2 = 123.9^0$ and was found to be -13.208 radians per square second, whereas the maximum value of its angular acceleration occurred at $\theta_2 = 291.2^0$ and was found to be 13.573 radians per square second. Thus, the angular acceleration of the swing jaw can attain substantial magnitudes.

A graph of the variation of α_3 with θ_2 is shown in Figure 15.

Table IX. Analytically determined values of α_3 for given values of θ_2

θ_2 (degrees)	α_3 (rad/s^2)	θ_2 (degrees)	α_3 (rad/s^2)
0	5.415	195	−3.315
15	2.362	210	0.543
30	−0.767	225	4.384
45	−3.820	240	7.858
60	−6.657	255	10.659
75	−9.175	270	12.573
90	−11.150	285	13.490
105	−12.538	300	13.406
120	−13.179	315	12.401
135	−12.960	330	10.617
150	−11.813	345	8.226
165	−9.741	360	5.415
180	−6.841		

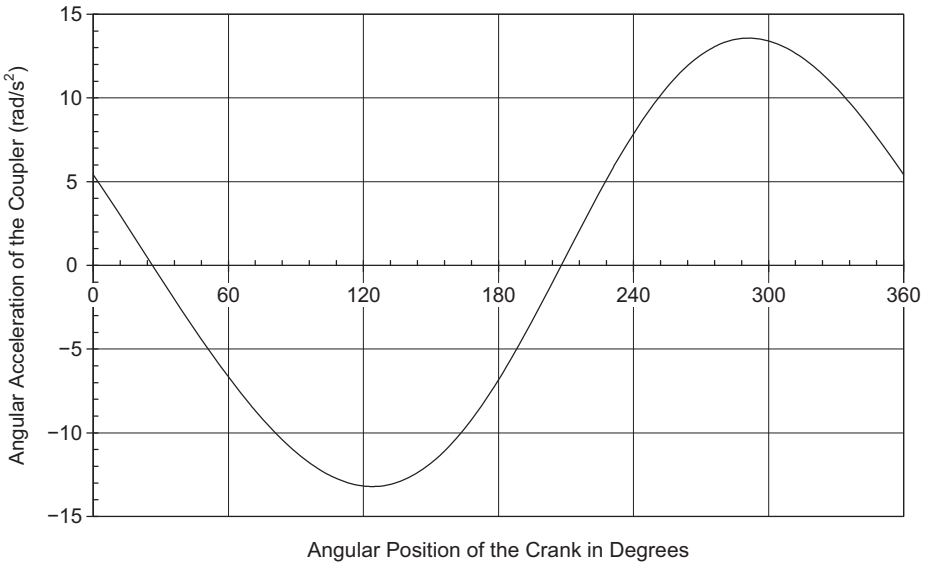

Figure 15. Angular accelerations of the coupler versus crank angle

Determination of the acceleration of a point in the swing jaw

For the values of r_5 given in Table III, the values of the acceleration components a_{PV} and a_{PH} were determined, using equation (35), for one complete cycle of motion of the mechanism. The data in Tables X and XI are representative of the results.

In Table X, negative values indicate an acceleration that is directed vertically downward and would either slow down the vertical component of velocity of the swing jaw, if it were moving in the upward direction, or speed up the vertical component of velocity of the swing jaw, if it were moving in the downward direction. Positive values indicate an acceleration that is directed vertically upward and would either slow down the vertical component of velocity of the swing jaw, if it were moving in the downward direction, or speed up the vertical component of velocity of the swing jaw, if it were moving in the upward direction. As can be seen in Table X, the maximum value of the component of acceleration in the Y direction increases monotonously, at a slightly increasing rate, as we move from point $P1$ through to $P5$.

Table X. Accelerations in the Y direction

Point	$P1$	$P2$	$P3$	$P4$	$P5$
$\ddot{y}_{min}$ (m/s^2)	−9.953	−10.467	−11.092	−11.817	−12.629
$\ddot{y}_{max}$ (m/s^2)	9.953	10.647	11.420	12.252	13.132

Table XI. Accelerations in the Z direction

Point	$P1$	$P2$	$P3$	$P4$	$P5$
$\ddot{z}_{min}$ (m/s^2)	−9.953	−8.993	−8.064	−7.176	−6.339
$\ddot{z}_{max}$ (m/s^2)	9.953	8.807	7.716	6.720	5.887

In Table XI, negative values indicate an acceleration that is directed horizontally away from the fixed jaw and would either slow down the horizontal component of velocity of the swing jaw, if it were moving towards the fixed jaw, or speed up the horizontal component of velocity of the swing jaw, if it were moving away from the fixed jaw. Positive values indicate an acceleration that is directed horizontally towards the fixed jaw and would either slow down the horizontal component of velocity of the swing jaw, if it were moving away from the fixed jaw, or speed up the horizontal component of velocity of the swing jaw, if it were moving towards the fixed jaw. As can be seen in Table XI, the maximum value of the component of acceleration in the Z direction decreases monotonously and at a slightly decreasing rate, as we move from point $P1$ through to $P5$.

The vertical components of acceleration for points $P1$ through to $P5$ are compared graphically in Figure 16, for one complete rotation of the crank.

It can be seen in Figure 15 that the angular velocity of the swing jaw instantaneously becomes zero when $\theta_2 \cong 26.32^0$ and when $\theta_2 \cong 207.92^0$. At these instances, the acceleration of the swing jaw becomes purely translational, and all the points in it have the same vertical component of acceleration, as can be seen in Figure 16.

The horizontal components of acceleration for points $P1$ through to $P5$ are compared graphically in Figure 17, for one complete rotation of the crank. Again, it can be seen in Figure 15 that the angular velocity of the swing jaw instantaneously becomes zero when $\theta_2 \cong 26.32^0$ and when $\theta_2 \cong 207.92^0$. At these instances, the acceleration of the swing jaw becomes purely translational, and all the points in it have the same horizontal (and vertical) component of acceleration, as can be seen in Figure 17.

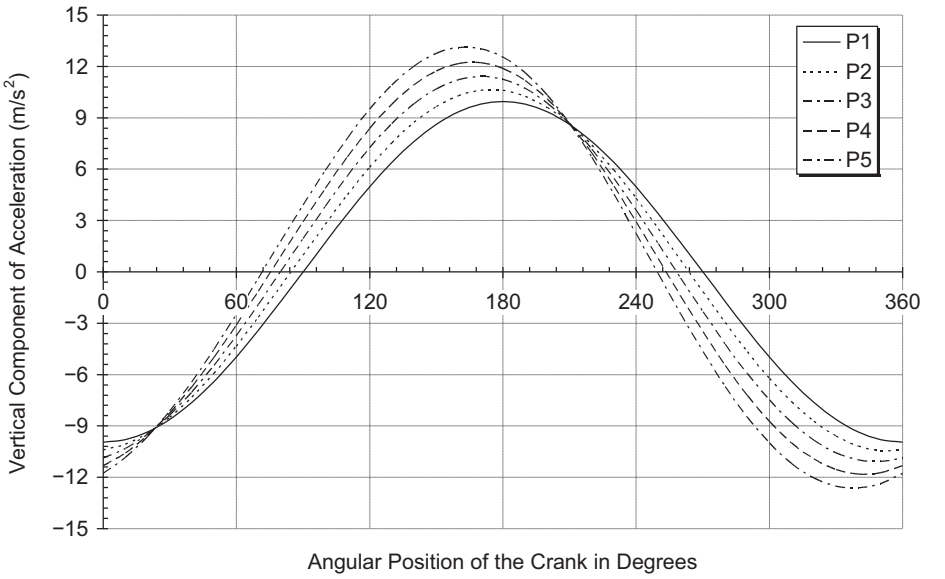

Figure 16.
Vertical components of acceleration of points in the swing jaw

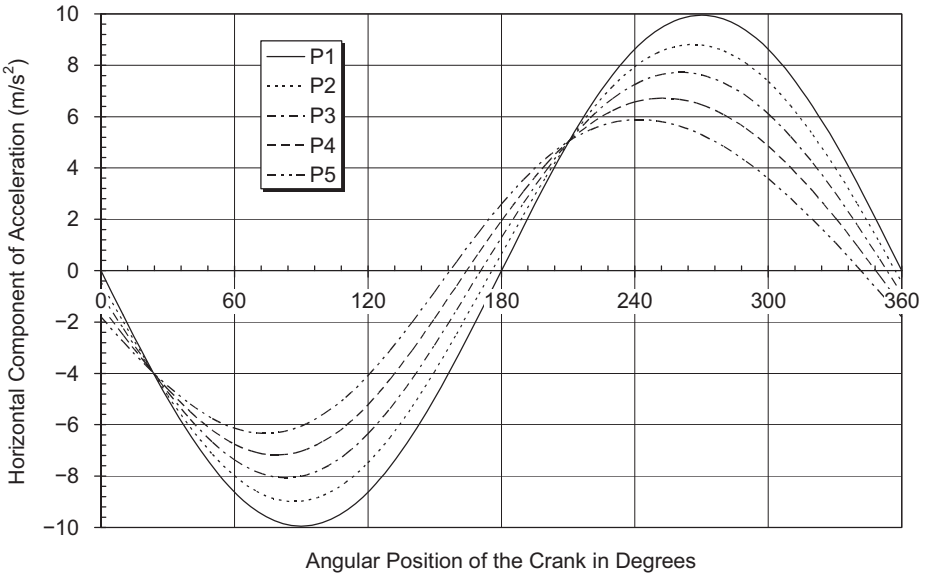

Figure 17. Horizontal components of acceleration of points in the swing jaw

Conclusions

The crushing mechanism of the single toggle jaw crusher can be modelled as a planar crank and rocker mechanism, with the eccentric shaft being modelled as a short crank, the swing jaw of the crusher being modelled as the coupler link and the toggle link being modelled as the rocker.

Starting with a suitable right-handed Cartesian coordinate reference frame, a unique kinematical model of the single toggle jaw crusher was established. The vector loop closure method and the differential calculus were then used to derive, from first principles, the equations of position, velocity and acceleration for any specified point in the swing jaw of the crusher. The method of kinematical analysis used here is not in itself new but, to the authors' knowledge, it has not been used before in the study of jaw crusher mechanics and the kinematical equations, as derived and presented in this paper, have not been presented elsewhere.

Application of the derived equations was demonstrated with the use of the dimensions of a practical single toggle jaw crusher. Further, it was demonstrated, with the aid of graphical plots, that the motion of the swing jaw of the single toggle jaw crusher would have both horizontal and vertical components, relative to the material being crushed. Thus, the swing jaw applies a compressive crushing force as well as a rubbing force upon the material being crushed. The downward, rubbing force increases the throughput of the crusher but also increases the rate of wear of the crushing surfaces of the jaws.

The equations derived in this paper can be used to investigate the effects of any alterations in the design of the crusher mechanism, upon its kinematics. Further, given the kinematical equations, a static force analysis of the mechanism can be carried out to determine the force transmission characteristics of the mechanism. Moreover, a dynamic force analysis can be carried out to determine the dynamic behaviour of the

mechanism. An understanding of the force transmission characteristics and the dynamic behaviour of the mechanism is essential for sound design of the crusher.

The methods used in this paper can be applied to other types of jaw crushers, such as the double toggle jaw crusher. A similar analysis of the double toggle jaw crusher, for instance, would then facilitate an objective evaluation of its performance, as compared to the single toggle jaw crusher.

References

AUBEMA Jaw Crushers (2013), "A brochure", available at: www.tlt.as/Undersider/documents/JawCrusher.pdf (accessed May 2013).

Cao, J., Rong, X. and Yang, S. (2006), "Jaw plate kinematical analysis for single toggle jaw crusher design", *International Technology and Innovation Conference, 2006, Section 1: Advanced Manufacturing Technology*, *Hangzhou*, pp. 62-66.

Carmichael, R.D. and Smith, E.R. (1962), *Mathematical Tables and Formulas*, Dover Publications Incorporated, New York, NY.

Carter, R.A. (1999), "New jaw crushers are reliable, affordable and transportable", Rock Products, available at: www.rockproducts.com/index.php/features/51-archives/1240.pdf (accessed May 2013).

Deepak, B.B.V.L. (2010), "Optimum design and analysis of (the) swinging jaw plate of a single toggle jaw crusher", A Master of Technology Thesis, Department of Mechanical Engineering, National Institute of Technology, Rourkela, Odisha, available at: www.scribd.com/doc/37399105/Deepak-Project-on-Jaw-Crusher (accessed May 2013).

Erdman, A.G. and Sandor, G.N. (1991), *Mechanism Design*, Prentice-Hall, London.

Garnaik, S.K. (2010), "Computer aided design of (the) jaw crusher", A Bachelor of Technology Thesis, Department of Mechanical Engineering, National Institute of Technology, Rourkela, Odisha, available at: http://ethesis.nitrkl.ac.in/1812/1/thesis_sobhan.pdf (accessed May 2013).

Gupta, A. and Yan, D.S. (2006), *Mineral Processing, Design and Operations: An Introduction. Chapter 4: Jaw Crushers*, Elsevier, Melbourne.

Ham, C.W., Crane, E.J. and Rogers, W.L. (1958), *Mechanics of Machinery*, 4th ed., McGraw-Hill Book, New York, NY.

Henan Hongxing Mining Machinery Company Limited (2013), available at: www.hxjqchina.com/UpLoadFile/01.pdf (accessed January 2013).

Kalnins, L.M. (2009), *Coordinate Systems*, Department of Earth Sciences, University of Oxford, Oxford, available at: www.earth.ox.ac.uk/~larak/MMES/CoordinateSystems.pdf (accessed July 2013).

Kimbrell, J.T. (1991), *Kinematics Analysis and Synthesis*, McGraw-Hill Incorporated, New York, NY.

Martin George, H. (1982), *Kinematics and Dynamics of Machines*, 2nd ed., McGraw-Hill Incorporated, New York, NY.

Mathcentre (2009), "Cartesian components of vectors", available at: www.mathcentre.ac.uk/resources/uploaded/mc-ty-cartesian1-2009-1.pdf (accessed July 2013).

MIT (2013), *Review B: Coordinate Systems*, Massachusetts Institute of Technology, Department of Physics, Massachusetts, available at: http://web.mit.edu/8.02t/www/materials/modules/ReviewB.pdf (accessed July 2013).

Monkova, K., Monka, P., Hloch, S. and Valicek, J. (2011), "Kinematic analysis of (the) quick-return mechanism in three various approaches", *Technical Gazette*, Vol. 18 No. 2, pp. 295-299, available at: hrcak.srce.hr/file/103770 (accessed May 2013).

Mular, A.L., Doug, N.H. and Barrat, D.J. (2002), *Mineral Processing Plant Design, Practice and Control: Proceedings*, Vol. 1, pp. 584-605, Society for Mining, Metallurgy and Exploration, Incorporated (SME), Colorado.

Pennsylvania Crusher Corporation (2006), *Handbook of Crushing*, available at: www.mne.eng.psu.ac.th/pdf/Handbook%20of%20Crushing2003.pdf (accessed July 2013).

SBM Mining and Construction Machinery (2013), "A brochure", available at: www.sbmchina.com/pdf/jaw_crusher.pdf (accessed May 2013).

Shigley, J.E. and Uicker, J.J. Jr. (1980), *Theory of Machines and Mechanisms*, McGraw-Hill Book Company, New York, NY.

The Institute of Quarrying Australia (2013), "Technical briefing paper no. 6: crusher selection III", available at: www.quarry.com.au/files/technical_papers/microsoft_word_-_technical_paper-no.6.doc.pdf

Zhong, L. and Chen, K. (2010), "Study on digital platform for jaw crusher design", *2010 International Conference on Mechanics Automation and Control Engineering, IEEE, NJ*.

Corresponding author
Moses Frank Oduori can be contacted at: foduori@uonbi.ac.ke